Heteronuclear Monoazadienyl Complexes, Isolobally Related to Cyclopentadienyl Compounds[1]

Olaf C. P. Beers, Michiel M. Bouman, Agatha E. Komen, Kees Vrieze, and Cornelis J. Elsevier*

Anorganisch Chemisch Laboratorium, Universiteit van Amsterdam, Nieuwe Achtergracht 166, 1018 WV Amsterdam, The Netherlands

Ernst Horn and Anthony L. Spek

Bijvoet Center for Biomolecular Research, Vakgroep Kristal- en Structuurchemie, Universiteit Utrecht, Padualaan 8, 3584 CH Utrecht, The Netherlands

Received July 31, 1992

The complex $Ru(CO)_3Cl\{RC{=}C(H)C(H){=}N\text{-}i\text{-}Pr\}$ (**2a**, R = Ph; **2b**, R = Me), which is isolobally related to C_5H_5Cl (Cp-Cl), has been used as a building block for the preparation of heteronuclear monoazadienyl (MAD-yl) complexes via reactions with $Co(CO)_4^-$, $Fe(CO)_2Cp^-$, and $Mn(CO)_5^-$. These reactions have afforded the new complexes $RuCo(CO)_6\{RC{=}C(H)C(H){=}N\text{-}i\text{-}Pr\}$ (**5**), $CpFeRu(CO)_4\{PhC{=}C(H)C(H){=}N\text{-}i\text{-}Pr\}$ (**6**), and $RuMn(CO)_8\{RC{=}C(H)C(H){=}N\text{-}i\text{-}Pr\}$ (**8**), all containing the ruthena-azadienyl cycle. The complexes have been characterized by IR and ^1H and ^{13}C NMR spectroscopy, and the structures of $RuCo(CO)_6\{MeC{=}C(H)C(H){=}N\text{-}i\text{-}Pr\}$ (**5b**) and $CpFeRu(CO)_4\{PhC{=}C(H)C(H){=}N\text{-}i\text{-}Pr\}$ (**6a**) have been determined by X-ray structure analyses. Crystals of **5b** are monoclinic, space group $P2_1/c$, with a = 7.127 (1) Å, b = 13.931 (1) Å, c = 16.536 (1) Å, β = 93.92 (1)°, and Z = 4. The structure was refined to R = 0.030 for 2978 observed reflections. Crystals of **6a** are monoclinic, space group $P2_1/c$, with a = 9.223 (1) Å, b = 11.243 (1) Å, c = 19.179 (4) Å, β = 103.18 (1)°, and Z = 4. The structure was refined to R = 0.048 for 2921 observed reflections. Upon thermolysis of complexes **5** and **6a**, featuring $\sigma(N),\sigma(C),\pi(C{=}C)$-coordinated MAD-yl ligands, a CO ligand is substituted by the $\pi(C{=}N)$ bond of MAD-yl, but the resulting complex is only stable in the FeRu case (complex **7**). Upon thermolysis or photolysis of the RuMn complex **8**, featuring a $\sigma(N),\sigma(C)$-coordinated MAD-yl ligand, one or two CO ligands are substituted by the π bonds of the MAD-yl ligand, yielding the $RuMn(CO)_7$- and $RuMn(CO)_6$(MAD-yl) complexes **9** and **10**, respectively. The reaction of **5a** and **8b** with I_2 as well as electrochemical measurements involving **7** show that the intermetallic bond in the new heteronuclear complexes is not stable toward oxidation. Complex **10a** is a hydrogenation catalyst for styrene, where the reversible hapticity change of the Mn-coordinated ruthena aza dienyl cycle from η^5 to η^3 and successively to η^1 has been proposed to be crucial for the uptake of the alkene and hydrogen by the catalyst.

Introduction

The cyclopentadienyl ligand is among the most frequently used ligands in organometallic chemistry nowadays, which is particularly due to its stabilizing effect on metal atoms in different oxidation states. Another aspect of Cp as a ligand is its intrinsic versatile coordination behavior, acting as a formally monoanionic two-, four-, or six-electron-donating ligand. If the hapticity of Cp is changed, one or more open sites can be created in the coordination sphere of the metal, thus providing one of the prerequisites for a catalytic reaction.[2] The specific properties of the Cp ligand are generally varied by the introduction of substituents such as methyl groups.

Recently, we have obtained the interesting new metallacyclic systems Ru—C=C—C=N from reactions of monoaza dienes $RC(H){=}C(H)C(H){=}NR'$ with $Ru_3(CO)_{12}$ (Figure 1),[3,4] in which the five-membered azaruthenacycle formed is isolobal with the Cp ligand.[4] By application of this isolobal analogy, the tetranuclear chain complex $Ru_4(CO)_{10}\{RC{=}C(H)C(H){=}NR'\}_2$ (**1**; Figure 1) may be regarded as an analogue of the complex $[CpRu(CO)_2]_2$.[3,4]

An excellent precursor for the introduction of the pseudo-Cp ligand $-(CO)_3RuC(R){=}C(H)C(H){=}N(R')-$ in other metal systems has been obtained from the oxidation reaction of **1b** (R = Me, R' = *i*-Pr) with CCl_4, Br_2, or I_2, which afforded the halogen-bridged dimer **2** (Figure 2).[5]

By subsequent reaction with CO, compound **2** could be converted into the mononuclear complex $Ru(CO)_3X\{MeC{=}C(H)C(H){=}N\text{-}i\text{-}Pr\}$ (**3b**), which may be considered as Cp-X by isolobal considerations. Substitution of X by metalates in principle would provide a direct route for the preparation of heteronuclear pseudo-cyclopentadienyl complexes. These complexes offer the possibility of studying the coordination properties of the pseudo-Cp ligand toward a variety of metal fragments. More generally, the interest in such heteronuclear compounds is derived from the unique reactivity that may arise as a result of the synergic effect of the constituent metals. Such

(1) Reactions of Monoazadienes with Metal Carbonyl Complexes. 15. For other parts see ref 3b.
(2) (a) O'Connor, J. M.; Casey, C. P. *Chem. Rev.* **1987**, *87*, 307. (b) Marx, D. E.; Lees, A. J. *Inorg. Chem.* **1988**, *27*, 1121.
(3) (a) Mul, W. P.; Elsevier, C. J.; Polm, L. H.; Vrieze, K.; Zoutberg, M. C.; Heijdenrijk, D.; Stam, C. H. *Organometallics* **1991**, *10*, 2247. (b) Elsevier, C. J.; Mul, W. P.; Vrieze, K. *Inorg. Chim. Acta* **1992**, *198-200*, 689.
(4) Polm, L. H.; Mul, W. P.; Elsevier, C. J.; Vrieze, K.; Christophersen, M. J. N.; Stam, C. H. *Organometallics* **1988**, *7*, 423.
(5) Mul, W. P.; Elsevier, C. J.; van Leijen, M.; Spaans, J. *Organometallics* **1991**, *10*, 251.

0276-7333/93/2312-0315$04.00/0

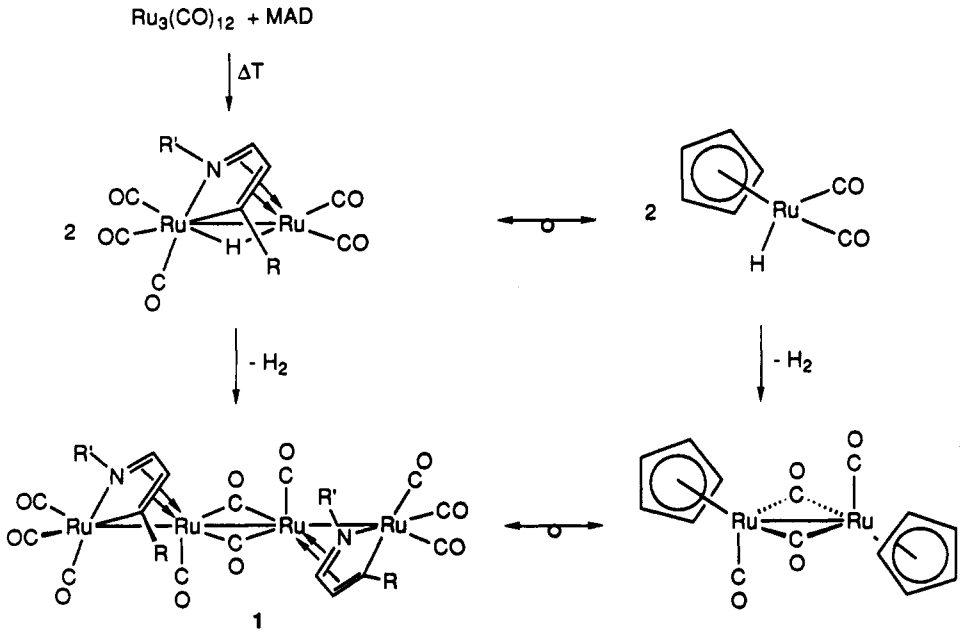

Figure 1. Isolobal analogy between Ru-monoazadienyl complexes and Ru-cyclopentadienyl complexes.

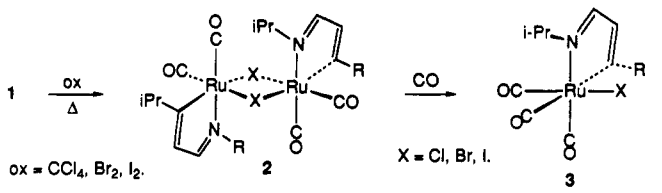

Figure 2. Oxidation of 1, affording complexes 2 and 3.

an effect has for example been demonstrated in the water-gas shift reaction, catalyzed by Fe/Ru carbonyls.[6]

This report deals with the preparation of new heteronuclear monoazadienyl complexes, using complex **3** as a building block in the reaction with three different metalates. Both $Co(CO)_4^-$ and $Mn(CO)_5^-$, d^7 and d^9 metals, respectively, have been chosen in order to evaluate the coordination behavior of the azaruthenacycle toward electronically very different metal fragments. From the reaction of **3** with the third metalate $Fe(CO)_2Cp^-$, a complex isolobally related to ferrocene with one real Cp and one pseudo-Cp ligand was anticipated, which would be attractive with respect to both structural and electrochemical properties in comparison with those of its isolobal analogue. Finally, an example of a hapticity change of the ruthena aza dienyl cycle as a prerequisite for a catalytic reaction will be reported.

Experimental Section

^1H and $^{13}C\{^1H\}$ NMR spectra were recorded on Bruker AC 100, WM 250, and AMX 300 spectrometers. The ^{13}C NMR spectra were recorded using an APT pulse sequence. IR spectra were measured on Perkin-Elmer 283 and Nicolet 7199B FTIR (liquid nitrogen cooled, Hg, Cd, Te detector) spectrophotometers using matched NaCl solution cells of 0.5-mm path length. Field desorption (FD) mass spectra were obtained with a Varian MAT711 double-focusing mass spectrometer with a combined EI/FI/FD source, fitted with a 10-μm tungsten-wire FD emitter containing carbon microneedles with an average length of 30 μm, using emitter currents of 0–15 mA. Elemental analyses were carried out by the elemental analysis section of the Institute for Applied Chemistry, TNO Zeist, The Netherlands, or Dornis und Kolbe, Mikroanalytisches Laboratorium, Mülheim a.d. Ruhr, Germany. All preparations were carried out under an atmosphere of purified nitrogen. Carefully dried solvents were used. Silica gel for column chromatography (Kieselgel 60, 70–230 mesh, E. Merck, Darmstadt, Germany) was dried before use. The complexes $Ru_4(CO)_{10}\{PhC{=}C(H)C(H){=}N\text{-}i\text{-}Pr\}_2$ (**1a**[3a]), $[Ru(CO)_2Cl\{MeC{=}C(H)C(H){=}N\text{-}i\text{-}Pr\}]_2$ (**2b**[5]), $KCo(CO)_4$, $KFe(CO)_2Cp$, and $KMn(CO)_5$[7] were prepared according to literature procedures. Reported FD mass data are based on the highest peak of the isotopic pattern of the molecular ion, which corresponds to ^{102}Ru and ^{56}Fe (calculated value in parentheses).

Synthesis of $[Ru(CO)_2Cl\{PhC{=}C(H)C(H){=}N\text{-}i\text{-}Pr\}]_2$ (2a). The employed procedure is analogous to the reported route to **2b**.[5] Because of the poor solubility of **1a** in heptane, the reaction of **1a** with CCl_4 was performed in toluene. When the reaction had run to completion (about 3–4 h), the solvent was evaporated and the residue chromatographed on silica. Elution with hexane/diethyl ether (9:1) afforded the yellow complex **2a** in 70% yield.

In Situ Preparation of $Ru(CO)_3\{RC{=}C(H)C(H){=}N\text{-}i\text{-}Pr\}^+OTf^-$ (4a, R = Ph; 4b, R = Me). A solution of 0.15 mmol of $[Ru(CO)_2Cl\{RC{=}C(H)C(H){=}N\text{-}i\text{-}Pr\}]_2$ (**2**; 110 mg of **2a** or 91 mg of **2b**) in 20 mL of dichloromethane (or THF) was stirred for 5 min under an atmosphere of CO. The solution of $Ru(CO)_3Cl\{RC{=}C(H)C(H){=}N\text{-}i\text{-}Pr\}$ (**3**) so prepared was stirred for 30 min with 0.08 g of AgOTf (0.3 mmol). The resulting suspension was filtered to remove AgCl. Complex **4** was characterized by IR spectroscopy of the filtrate (cm^{-1}): **4a** (CH_2Cl_2), 2120 (s), 2070 (s), 2035 (s); **4a** (THF), 2054 (s), 1985 (vs); **4b** (CH_2Cl_2), 2120 (s), 2110 (s), 2055 (s); **4b** (THF), 2051 (s), 1982 (vs).

Synthesis of $RuCo(CO)_6\{RC{=}C(H)C(H){=}N\text{-}i\text{-}Pr\}$ (5a, R = Ph; 5b, R = Me). To a solution of 0.30 mmol of **4** in 20 mL of CH_2Cl_2 (or THF), obtained as described above, was slowly added at −78 °C a solution of 0.2 g of $KCo(CO)_4$ (about 3 equiv) in 10 mL of CH_2Cl_2 (or THF). Instantaneously the solution changed from yellow to red-brown. The solution was stirred for 1 h, while it was gradually warmed to 20 °C. Then the solvent was evaporated and the product chromatographed on silica. Elution with hexane/diethyl ether (20:1) afforded a dark red fraction, containing 93 mg of **5a** (62%) or 71 mg of **5b** (54%). Complex **5** was recrystallized from hexane at −80 °C; crystals of **5b**, suitable for X-ray crystallography, were obtained from a concentrated hexane solution at −20 °C. Anal. Found (calcd) for $C_{13}H_{12}NO_6CoRu$ (**5b**): C, 35.22 (35.63); H, 3.06 (2.76); N, 3.01 (3.20). FD mass for **5a**: *m/e* 501 ($M^{\cdot+}$ = 501).

(6) Ungermann, C.; Landis, V.; Moya, S. A.; Cohen, H.; Walker, H.; Pearson, R. G.; Rinker, R. G.; Ford, P. C. *J. Am. Chem. Soc.* **1979**, *101*, 5922.

(7) Ellis, J. E.; Flom, E. A. *J. Organomet. Chem.* **1975**, *99*, 263.

Synthesis of $(\eta^5\text{-}C_5H_5)FeRu(CO)_4\{PhC{=}C(H)C(H){=}N\text{-}i\text{-}Pr\}$ (6a). A solution of about 1 equiv of $KFe(CO)_2Cp$ in 20 mL of THF was slowly added by means of a dropping funnel at −78 °C to a solution of 0.30 mmol of **4a** in 30 mL of THF, obtained as described above. An instantaneous reaction was observed by the immediate color change from yellow to dark brown. After the mixture was gradually warmed to 20 °C (about 1 h), the solvent was evaporated and the residue brought on top of a silica column. Upon elution with hexane/diethyl ether (9:1), a brown-red fraction was obtained, containing 41 mg of complex **6a** (27%). Subsequent elution with hexane/diethyl ether (4:1) yielded a brown fraction, containing considerable amounts of $[CpFe(CO)_2]_2$. Anal. Found (calcd) for $C_{21}H_{19}NO_4FeRu$ (**6a**): C, 49.90 (49.82); H, 3.90 (3.78); N, 2.75 (2.77). FD mass: *m/e* 507 ($M^{\bullet+}$ = 507).

Synthesis of $RuMn(CO)_8\{RC{=}C(H)C(H){=}N\text{-}i\text{-}Pr\}$ (8). (i) Under CO. To a solution of 0.30 mmol of **4** in 30 mL of THF, prepared as described above, was slowly added a solution of about 1.5 equiv of $KMn(CO)_5$ in 15 mL of THF at −80 °C under a CO atmosphere. Instantaneously, the solution changed from yellow to red. After the mixture was gradually warmed to 20 °C (about 1 h), the solvent was evaporated and the residue chromatographed on silica. With hexane as the eluent, a small amount of $Mn_2(CO)_{10}$ was eluted. Upon subsequent elution with hexane/CH_2Cl_2 (20:1), an orange-yellow fraction was obtained, containing complex **8** (**8a**, 92 mg, 56%; **8b**, 91 mg, 62%). Anal. Found (calcd) for $C_{15}H_{12}NO_8RuMn$ (**8b**): C, 36.77 (36.75); H, 2.52 (2.47); N, 2.94 (2.86). FD mass for **8a**: *m/e* 553 ($M^{\bullet+}$ = 553).

(ii) Under N_2. When the same procedure was followed as described above, but now under an inert atmosphere, a mixture of complexes **8**–**10** was obtained. All three complexes were eluted with hexane/CH_2Cl_2 ((20–10):1), so by this route the complexes were not obtained separately. The total yield of heteronuclear compounds was about 60%. The spectroscopic data for complex **9** (Tables VI–VIII) were deduced from the spectra of this mixture.

Thermal Reaction of 5. A solution of 0.1 mmol of **5a**/**5b** in 20 mL of heptane was stirred at 100 °C for 4 h. The IR spectrum of the reaction mixture showed the presence of five new absorption bands at 2079 (s), 2013 (s), 2000 (vs), 1991 (s), and 1945 (m, br) cm^{-1} for **5a** and at 2072 (s), 2005 (s), 1998 (vs), 1987 (s), and 1940 (s) cm^{-1} for **5b**. Upon purification of this crude product by column chromatography on silica, total decomposition took place. Attempts to measure NMR spectra of the unpurified product resulted in very broad resonances. When the heptane solution of the thermal product of **5a**/**5b** was stirred under a CO atmosphere at 20 °C, instantaneously complex **5a**/**5b** was formed back.

Thermal Conversion of 6a into $(\eta^5\text{-}C_5H_5)FeRu(CO)_3\{PhC{=}C(H)C(H){=}N\text{-}i\text{-}Pr\}$ (7a). A solution of 50 mg of **6a** (0.1 mmol) in 15 mL of heptane was stirred at reflux. After 1 h the reaction had run to completion, as monitored by IR spectroscopy and by a color change from brown to red. After purification by column chromatography on silica, using hexane/CH_2Cl_2 (4:1) as the eluent, complex **7a** was obtained in 92% yield (44 mg). Complex **7a** could be recrystallized as dark red needles from a concentrated methanol solution at −80 °C. Anal. Found (calcd) for $C_{20}H_{19}NO_3FeRu$ (**7a**): C, 50.20 (50.22); H, 4.05 (4.00); N, 3.11 (2.93). FD mass: *m/e* 479 ($M^{\bullet+}$ = 479).

In an attempt to effect the reverse reaction, a solution of 48 mg of **7a** (0.1 mmol) in 20 mL of heptane was stirred under 1.2 bar of CO at 100 °C for 4 h. Monitoring the reaction by IR indicated that no reaction took place. Also, when a solution of 14 mg of **7a** (0.03 mmol) in 3 mL of hexane in a sapphire tube under 8 bar CO was irradiated with a high-pressure Hg lamp for 1 h, no conversion was realized either.

Thermal Conversion of 8 into $RuMn(CO)_6\{RC{=}C(H)C(H){=}N\text{-}i\text{-}Pr\}$ (10). (i) A solution of 55 mg of **8a** (0.1 mmol) in 20 mL of heptane was stirred for 1 h at 60 °C. No change in the IR spectrum of the reaction mixture was observed. Therefore, the temperature was raised to 100 °C. After 10 min of reaction time IR spectroscopy indicated about 30% conversion into **10a** and the presence of a small amount of **9a**. After 1 h at 100 °C the reaction was stopped and the solvent of the resulting clear orange-yellow solution evaporated, affording the pure complex **10a** (49 mg, 98%). Anal. Found (calcd) for $C_{18}H_{14}NO_6RuMn$ (**10a**): C, 43.42 (43.56); H, 2.89 (2.84); N, 2.70 (2.82). FD mass: *m/e* 497 ($M^{\bullet+}$ = 497).

(ii) When the mixture of complexes **8**–**10**, obtained from the reaction of **4** with $KMn(CO)_5$ under N_2, was treated as described above, the pure complexes **10a** and **10b** were obtained quantitatively as well. In an attempt to realize the reverse reaction, a solution of 0.1 mmol of **10a** in 20 mL of heptane was stirred under a CO atmosphere under variable reaction conditions (1 bar of CO/20 °C; 1 bar of CO/100 °C; 35 bar of CO/50 °C; 50 bar of CO/75 °C). No reaction was observed.

Photochemical Conversion of 8a. A solution of 55 mg of **8a** (0.1 mmol) in 30 mL of heptane was irradiated with a high-pressure Hg lamp for 15 min. Both ^1H NMR and IR spectroscopy revealed the presence of complex **9a**. Considerable amounts of $Mn_2(CO)_{10}$ were detected in the IR spectrum. Upon prolonged irradiation, all heteronuclear complexes decomposed and only $Mn_2(CO)_{10}$ could be isolated.

Reactivity of 5a and 8b toward I_2. To a solution of 0.1 mmol of **5a** or **8b** in 10 mL of CH_2Cl_2 was added through a dropping funnel a CH_2Cl_2 solution of 0.2 mmol of I_2 (about 0.01 M) at 20 °C. Immediate discoloring after addition of I_2 indicated an instantaneous reaction. The reaction was stopped when the dark color of I_2 no longer faded. The IR spectrum of the reaction mixture showed the absorption bands of complex **3a** or **3b** (Table VI). After evaporation of the solvent the residue was purified by chromatography on silica. Elution with hexane/CH_2Cl_2 (10:1) afforded complex **2a** or **2b** (X = I), according to ^1H NMR and IR spectroscopy.

Electrochemical Measurements. Cyclic voltammetric measurements were carried out with a PAR Model 173 potentiostat, equipped with a PAR Model 176 I/E converter coupled to a PAR Model 175 universal programmer. Normal and differential pulse voltammograms were recorded at a scan rate of 5 mV/s with a pulse frequency of 2 pulses per second. Platinum working and auxiliary electrodes were used. An Ag^+/Ag (0.1 M AgOTf) reference electrode was employed in THF and a commercial Ag/AgCl reference electrode in acetone. The half-wave potential of a 10^{-3} M solution of ferrocene (Fc) was measured under the same experimental conditions: $E_{1/2}$ = −0.203 V in THF and $E_{1/2}$ = 0.641 V in acetone. The supporting electrolyte was 0.1 M Bu_4NPF_6 in both THF and acetone. Controlled-potential electrolysis was carried out with a PAR Model 273 potentiostat.

Reactivity of 8 and 10 toward H_2. When a solution of 50 mg of **10a** (0.1 mmol) in 20 mL of heptane was stirred under varying reaction conditions (1 bar of H_2/20 °C; 1 bar of H_2/100 °C; 40 bar of H_2/45 °C), no reaction was observed. Decomposition occurred after about 4 h of reaction time, employing 50 bar of H_2 and 50 °C.

When a solution of 0.1 mmol of **8b** in 20 mL of heptane was stirred under a H_2 atmosphere at 50 °C for 3 h, IR spectroscopy indicated the disappearance of **8b** and formation of $Mn_2(CO)_{10}$. ^1H NMR revealed the formation of small amounts of $H_4Ru_4(CO)_{12}$ and traces of $HRu_2(CO)_5\{MeC{=}C(H)C(H){=}N\text{-}i\text{-}Pr\}$ by their characteristic resonances at low frequency (−17.9[8] and −9.8 ppm,[9] respectively).

Catalytic Hydrogenation of Alkenes, Catalyzed by 10a. (i) Styrene. A solution of 50 mg of **10a** (0.1 mmol) in neat styrene (1.0 g, 10 mmol, 100 equiv) was stirred under 1.2 bar of H_2 at 100 °C for 16 h. Examination of the crude reaction mixture by $^1H/^{13}C$ NMR spectroscopy indicated the complete conversion of styrene into ethylbenzene. Complex **10a** could be recovered by purification of the reaction mixture by column chromatography on silica. The experiment could be repeated with the complex **10a** recovered.

(8) Knox, S. A. R.; Koepke, J. W.; Andrews, M. A.; Kaesz, H. D. *J. Am. Chem. Soc.* **1975**, *97*, 3942.
(9) Mul, W. P.; Elsevier, C. J.; Van Leijen, M.; Vrieze, K.; Smeets, W. J. J.; Spek, A. L. *Organometallics* **1992**, *11*, 1877.

Table I. Crystal Data and Details of the Structure Determination of 5b and 6a

	5b	6a
	Crystal Data	
formula	$C_{13}H_{12}NO_6CoRu$	$C_{21}H_{19}NO_4FeRu$
mol wt	438.24	506.30
cryst syst	monoclinic	monoclinic
space group	$P2_1/c$ (No. 14)	$P2_1/c$ (No. 14)
a, Å	7.127 (1)	9.2234 (10)
b, Å	13.931 (1)	11.2432 (10)
c, Å	16.536 (1)	19.179 (4)
β, deg	93.92 (1)	103.185 (10)
V, Å^3	1638.0 (3)	1936.4 (5)
D_{calc}, g/cm^3	1.777	1.737
Z	4	4
F(000), electrons	864	1016
μ, cm^{-1}	19.4	15.4
cryst size, mm	0.62 × 0.27 × 0.13	0.30 × 0.40 × 0.40
	Data Collection	
temp, K	295	100
radiation	Mo Kα (Zr), 0.710 73 Å	Mo Kα (Zr), 0.710 73 Å
$\theta_{min}/\theta_{max}$, deg	1.24, 27.5	1.0, 27.5
scan type	$\omega/2\theta$	$\omega/2\theta$
$\Delta\omega$, deg	0.60 + 0.35 tan θ	1.77 + 0.35 tan θ
horiz and vert aperture, mm	3.00, 6.00	3.00, 5.00
ref reflns	−1,0,−2; 220; 043	−1,−1,0; −3,0,4; 0,4,−2
data set	−9 to 0, 0−18, −21 to +21	−11 to 0, 0 to −14, −24 to +24
total no. of data	4221	9862
no. of unique data	3748	4418
no. of obsd data ($I > 2.5\sigma(I)$)	2981	2921
	Refinement	
N_{ref}, N_{par}	2978, 237	2921, 226
R, R_w, S	0.0300, 0.0320, 0.99	0.0479, 0.0469, 2.99
weighting scheme	$1/\sigma^2(F)$	$w^{-1} = \sigma^2(F) + 0.000137(F)^2$
max and av shift error	0.40, 0.03	0.38, 0.04
max/min residual density, e Å^{-3}	−0.60, 0.51	−1.12, 0.88

(ii) α-Methylstyrene. When the experiment described for styrene was carried out with α-methylstyrene under the same conditions, NMR spectroscopy of the reaction mixture revealed that no hydrogenation had taken place. Again complex **10a** was completely recovered.

(iii) 1-Octene. After 1-octene was employed as the alkene under the circumstances described for styrene, the reaction mixture was examined with $^1H/^{13}C$ NMR spectroscopy and GC. These methods showed that no hydrogenation had taken place and 1-octene was still 53% unconverted. The remaining part appeared to be isomerized to (*E*)-2-octene (27%), (*Z*)-2-octene (15%), and (*E*)-3-octene (5%).

Crystal Structure Determination of 5b and 6a. X-ray data were collected on an Enraf-Nonius CAD4 diffractometer. Crystal data are collected in Table I. Both structures were solved with the PATT option of SHELXS86[10] and refined on F by full-matrix least-squares techniques with SHELX76.[11] Neutral atom scattering factors were taken from ref 12 and corrected for anomalous dispersion.[13] The programs PLATON and PLUTON of the EUCLID package[14] were used for the geometrical calculations and molecular graphics. All calculations were done on a MicroVAX cluster. Positional parameters are listed in Tables II and III.

Table II. Final Coordinates and Equivalent Isotropic Thermal Parameters for the Non-Hydrogen Atoms of 5b

atom	x	y	z	U(eq),[a] Å^2
Ru	0.14763 (4)	0.09047 (2)	0.28178 (1)	0.0384 (1)
Co	0.12179 (7)	0.21760 (3)	0.16037 (3)	0.0449 (1)
O(1)	0.2138 (5)	0.41117 (19)	0.11260 (18)	0.0814 (11)
O(2)	−0.1734 (5)	0.1696 (2)	0.03586 (18)	0.0994 (14)
O(3)	−0.0632 (4)	0.29774 (17)	0.29379 (16)	0.0631 (9)
O(4)	−0.2105 (4)	−0.00072 (19)	0.20925 (17)	0.0818 (11)
O(5)	−0.0313 (4)	0.1248 (2)	0.44558 (16)	0.0809 (13)
O(6)	0.3374 (5)	−0.09774 (18)	0.33052 (19)	0.0868 (11)
N(1)	0.4032 (3)	0.16646 (18)	0.30923 (14)	0.0415 (8)
C(1)	0.4883 (5)	0.2035 (3)	0.3870 (2)	0.0505 (11)
C(2)	0.5072 (6)	0.1249 (3)	0.4501 (3)	0.0622 (14)
C(3)	0.3767 (7)	0.2888 (3)	0.4154 (3)	0.0705 (17)
C(4)	0.4755 (5)	0.1927 (2)	0.2436 (2)	0.0514 (11)
C(5)	0.3974 (5)	0.1576 (3)	0.1666 (2)	0.0534 (11)
C(6)	0.2547 (5)	0.0897 (2)	0.16756 (19)	0.0523 (11)
C(7)	0.2274 (8)	0.0128 (3)	0.1030 (3)	0.0772 (18)
C(8)	0.1806 (5)	0.3348 (3)	0.1322 (2)	0.0556 (12)
C(9)	−0.0551 (6)	0.1853 (3)	0.0831 (2)	0.0623 (14)
C(10)	0.0195 (5)	0.2511 (2)	0.2505 (2)	0.0464 (11)
C(11)	−0.0761 (5)	0.0315 (2)	0.2385 (2)	0.0537 (11)
C(12)	0.0370 (5)	0.1145 (2)	0.3870 (2)	0.0517 (11)
C(13)	0.2655 (5)	−0.0276 (3)	0.3124 (2)	0.0540 (11)

[a] U(eq) = one-third of the trace of the orthogonalized U.

Table III. Final Coordinates and Equivalent Isotropic Thermal Parameters for the Non-Hydrogen Atoms of 6a

atom	x	y	z	U(eq),[a] Å^2
Ru(1)	1.18451 (6)	0.22807 (5)	0.00384 (3)	0.0097 (1)
Fe(1)	1.36853 (9)	0.21999 (9)	−0.08638 (4)	0.0110 (3)
O(1)	0.8647 (5)	0.2849 (5)	0.0101 (3)	0.0275 (17)
O(2)	1.1237 (5)	−0.0258 (4)	−0.0469 (3)	0.0214 (16)
O(3)	1.2911 (6)	0.1248 (4)	0.1573 (3)	0.0246 (17)
O(4)	1.5564 (5)	0.2444 (4)	0.0568 (2)	0.0189 (14)
N(1)	1.2605 (6)	0.4068 (5)	0.0259 (3)	0.0131 (17)
C(1)	0.9850 (7)	0.2648 (6)	0.0093 (3)	0.0174 (17)
C(2)	1.1456 (7)	0.0720 (6)	−0.0285 (4)	0.0182 (19)
C(3)	1.2543 (7)	0.1670 (6)	0.1014 (4)	0.0165 (19)
C(4)	1.4672 (7)	0.2385 (7)	0.0027 (3)	0.0180 (19)
C(5)	1.2935 (7)	0.4535 (6)	−0.0302 (3)	0.0128 (19)
C(6)	1.2624 (7)	0.3871 (6)	−0.0975 (3)	0.0124 (17)
C(7)	1.1640 (7)	0.2892 (5)	−0.1004 (3)	0.0116 (17)
C(8)	1.0470 (6)	0.2644 (6)	−0.1664 (3)	0.0122 (17)
C(9)	0.9341 (7)	0.1812 (6)	−0.1672 (3)	0.0163 (17)
C(10)	0.8268 (7)	0.1585 (6)	−0.2296 (4)	0.021 (2)
C(11)	0.8249 (8)	0.2189 (7)	−0.2931 (4)	0.0264 (19)
C(12)	0.9353 (8)	0.3043 (7)	−0.2927 (4)	0.025 (2)
C(13)	1.0430 (7)	0.3268 (6)	−0.2302 (3)	0.0167 (19)
C(14)	1.2837 (8)	0.4789 (6)	0.0923 (3)	0.0159 (19)
C(15)	1.4212 (7)	0.4378 (6)	0.1471 (3)	0.018 (2)
C(16)	1.1433 (8)	0.4774 (6)	0.1216 (4)	0.023 (2)
C(171)[b]	1.3189 (17)	0.0886 (14)	−0.1659 (9)	0.035 (6)
C(181)[b]	1.3672 (16)	0.1934 (13)	−0.1929 (6)	0.024 (4)
C(191)[b]	1.5148 (17)	0.2164 (11)	−0.1541 (8)	0.024 (4)
C(201)[b]	1.5516 (13)	0.1269 (13)	−0.1028 (7)	0.023 (4)
C(211)[b]	1.4305 (18)	0.0536 (13)	−0.1125 (8)	0.027 (5)

[a] U(eq) = one-third of the trace of the orthogonalized U. [b] Site occupancy factor of these atoms is equal to 0.62.

(i) Complex 5b. Data were collected for a brown-red crystal mounted on top of a glass fiber. Unit cell parameters were determined from a least-squares treatment of the SET4 setting angles of 25 reflections with $14 < \theta < 18°$. The intensities of 4221 reflections were corrected for Lp and for absorption/extinction (using the DIFABS method;[15] correction range 0.89–1.31; consistent with variations observed in 360° ψ scans). H atoms were located from a difference Fourier map and their positions refined. All non-hydrogen atoms were refined with anisotropic thermal parameters.

(ii) Complex 6a. Data were collected at 100 K for a brownish crystal glued on top of a glass fiber. Unit cell parameters were

(10) Sheldrick, G. M. SHELXS86, Program for Crystal Structure Determination; University of Göttingen: Göttingen, Federal Republic of Germany, 1986.
(11) Sheldrick, G. M. SHELX76, Crystal Structure Analysis Package; University of Cambridge, Cambridge, England, 1976.
(12) Cromer, D. T.; Mann, J. B. *Acta Crystallogr.* **1968**, *A24*, 321.
(13) Cromer, D. T.; Liberman, D. *J. Chem. Phys.* **1970**, *53*, 1891.
(14) Spek, A. L. The EUCLID Package. In *Computational Crystallography*; Sayre, D., Ed.; Clarendon Press: Oxford, 1982; p 528.
(15) Walker, N.; Stuart, D. *Acta Crystallogr.* **1983**, *A39*, 158.

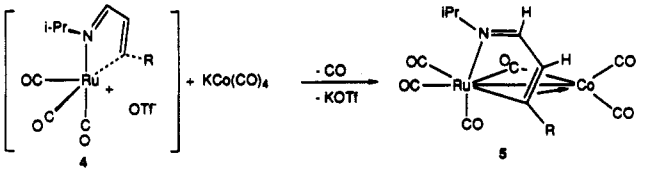

Figure 3. Formation of complex 5.

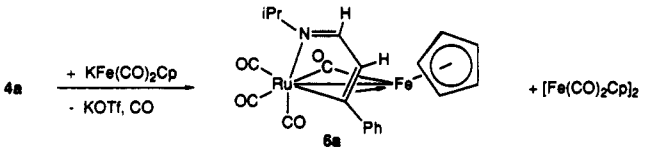

Figure 4. Formation of complex 6a.

determined from a least-squares treatment of the SET4 setting angles of 25 reflections in the range $12 < \theta < 18°$. The intensities of 9862 reflections were corrected for Lp and for absorption/extinction (using the DIFABS method;[15] correction range 0.9–1.2; consistent with variations observed in 360° ψ scans). H atoms were introduced on calculated positions and included in the refinement riding on their carrier atoms. All non-hydrogen atoms were refined with anisotropic thermal parameters except for the cyclopentadienyl ring (the disordered ring was modeled in two orientations with site occupancies 0.62 and 0.38).

Results and Discussion

Formation of the Heteronuclear Complexes 5, 6a, and 8. The synthesis of the heteronuclear complexes 5, 6a, and 8 was accomplished by the method of substitution of an anionic leaving group by a metalate. Five possible reaction routes for the interaction of metal carbonyl anions with complex metal halides have been suggested by Dessy et al.[16] The outcome of the reaction appears to be dependent on the nucleophilicity of the metalate, the order in which reactants are mixed, and the counterion of the employed metalate.

In order to incorporate the ruthena-azadienyl cycle in new heterometallic complexes, we considered complex 3 as a useful starting compound for the anionic substitution reaction. First we employed the mildly nucleophilic $Co(CO)_4^-$ [17] as the carbonylmetalate in the reaction with 3. Direct reaction between both reactants only occurred at elevated temperatures (±50 °C), and the yield of complex 5 was low. After complex 3 was activated for nucleophilic attack by abstracting the chloride with AgOTf, yielding in situ the cationic complex 4 (which was only characterized by IR spectroscopy), the reaction with $Co(CO)_4^-$ could be performed at low temperature and complex 5 was obtained in reasonable yields (±60%) (Figure 3). No formation of homometallic complexes was observed, which points to a nucleophilic substitution mechanism.[16]

In the reaction of the metalate $CpFe(CO)_2^-$ with the activated complex 4 only moderate amounts (27%) of the heteronuclear complex 6a were formed (Figure 4). Considerable quantities, however, of the dimer $[CpFe(CO)_2]_2$ were obtained as well, which points to a dominant reaction route involving single electron transfer instead of M–M' bond formation.[18] The $CpFe(CO)_2^-$ species then transfers one electron to the cationic Ru center, forming two radical

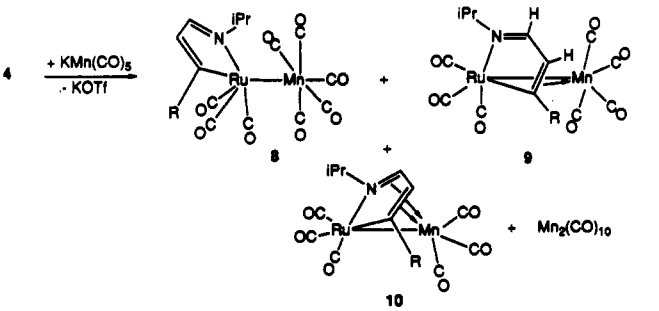

Figure 5. Formation of complexes 8–10.

intermediates. Provided a cage process occurs, the product from electron transfer may still be the desired heteronuclear complex 6a. Depending on the stability of the radical intermediates involved, the radicals may diffuse and recombine to give the homometallic species. Due to the strong nucleophilicity of $CpFe(CO)_2^-$,[17] the corresponding radical $^{\bullet}CpFe(CO)_2$ can be expected to be relatively stable, thus affording a large amount of the homonuclear dimer $[CpFe(CO)_2]_2$. The Ru-containing homonuclear dimer, which is the other expected byproduct, has, however, been neither isolated nor observed. This is in contrast, for example, to the reaction of $CpFe(CO)_2^-$ with $Mn(CO)_3$(*t*-Bu-DAB)Br, where no heteronuclear product was formed but both homometallic dimers could be isolated.[19]

From the reaction of 4 with the less nucleophilic anion $Mn(CO)_5^-$ [17] three products were isolated, viz. the complexes 8–10, which unfortunately could not be separated by column chromatography on silica (Figure 5). The complexes 8–10 appeared to represent three of the four possible π-coordination stages of the monoazadienyl ligand, as could be inferred from the spectroscopic data[20] (vide infra). The heteronuclear metal bond formation reaction could be further controlled by performing the reaction under an atmosphere of CO. Then, only complex 8 containing a σ(N),σ(C)-chelating monoazadienyl ligand was formed, which is quite remarkable in a metal–metal-bonded monoazadienyl complex. The only example of such a situation has been encountered in the reaction of $Ru_4(CO)_{10}\{MeC{=}C(H)C(H){=}N\text{-}i\text{-}Pr\}_2$ with CO at room temperature, where after a long reaction time (12 days) the system has been proposed to end up in a completely unbridged tetranuclear chain compound, featuring two chelating monoazadienyl ligands.[23] During the formation of 8 also a small amount of the homonuclear dimer $Mn_2(CO)_{10}$ was formed, thus lowering the total yield of heteronuclear complex to about 60%. The presence of $Mn_2(CO)_{10}$ points again to a single-electron-transfer (SET) mechanism, possibly in combination with a nucleophilic substitution pathway.[16]

Thermal and Photochemical Reactivity of 5, 6a, and 8. In order to obtain more insight into the coordination

(16) (a) Dessy, R. E.; Weissman, P. M. *J. Am. Chem. Soc.* **1966**, *88*, 5124. (b) Dessy, R. E.; Weissman, P. M. *J. Am. Chem. Soc.* **1966**, *88*, 5129.

(17) Pearson, R. G.; Figdore, P. E. *J. Am. Chem. Soc.* **1980**, *102*, 1541.

(18) Another possible reaction route involves a substitution reaction, yielding complex 6a, followed by a redistribution reaction with another molecule of $Fe(CO)_2Cp^-$,[16b] affording the dimer $[Fe(CO)_2Cp]_2$ and a $Ru(CO)_3\{PhC{=}C(H)C(H){=}N\text{-}i\text{-}Pr\}^-$ anion. The latter anion is probably unstable and decomposes.

(19) Keijsper, J.; van Koten, G.; Vrieze, K.; Zoutberg, M. C.; Stam, C. H. *Organometallics* **1985**, *4*, 1306.

(20) Only the π(C=N) coordination mode was not observed. This mode has until now never been observed in any isolated monoazadienyl complex. It has, however, been proposed as an intermediate in the photochemical reaction of 1 (Figure 1) with CO.[23]

(21) Crichton, O.; Rest, A. J.; Taylor, D. J. *J. Chem. Soc., Dalton Trans.* **1980**, 167.

(22) Belmont, J. A.; Wrighton, M. S. *Organometallics* **1986**, *5*, 1421.

(23) Mul, W. P.; Elsevier, C. J.; Vrieze, K.; Smeets, W. J. J.; Spek, A. L. *Organometallics* **1992**, *11*, 1891.

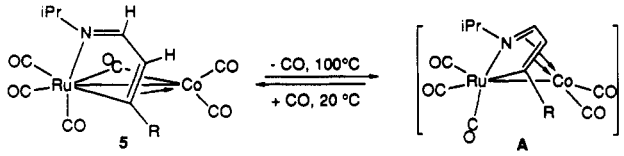

Figure 6. Thermal reaction of **5**, affording complex A.

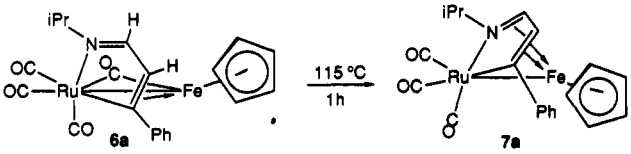

Figure 7. Thermal conversion of complex **6a** into **7a**.

behavior of the ruthena aza dienyl cycle toward the Co(CO)$_3$, Fe(CO)Cp, and Mn(CO)$_5$ fragments, we investigated the thermal reaction of **5**, **6a**, and **8**. When a solution of **5** in heptane was heated at reflux for 4 h, complete conversion with loss of CO took place to afford the new complex RuCo(CO)$_5${RC=C(H)C(H)=N-*i*-Pr} (A; Figure 6), which has been characterized solely on the basis of its IR spectrum (vide infra).

As a consequence of the loss of CO, the ligand system in complex A must be in the seven-electron-donating coordination mode with both π bonds attached to Co. Unfortunately, A is too reactive to be purified by column chromatography, and purification by filtration did not afford an appropriate sample for NMR spectroscopy either. As could be expected from a complex such as A, featuring a very reactive Co center, an instantaneous reaction took place with CO already at 20 °C, forming complex **5** back again. This reaction provides further support for the identity of A being RuCo(CO)$_5${RC=C(H)C(H)=N-*i*-Pr}, where the monoazadienyl ligand is σ(N),σ(C),π(C=C),π-(C=N) coordinated. Whereas η^3 coordination of the ruthena-azadienyl cycle toward a Co-carbonyl fragment appears to be thermodynamically more stable than η^5 coordination, this situation is reversed in the isolobally related cyclopentadienyl complexes. The complex Co(CO)$_3$(η^3-Cp) could only be observed at 12 K, upon photolysis of Co(CO)$_2$(η^5-Cp) in a CO matrix.[21]

In the case of the FeRu complex **6a**, thermal reaction under the same circumstances as for **5** actually yielded the stable complex **7a** (Figure 7), which could be completely characterized by spectroscopic and analytical methods (vide infra). In contrast to the RuCo complex A, complex **7a** could be neither thermally nor photochemically reconverted into **6a** by reaction with CO. This is an indication of the strong bonding interaction of the azaruthenacycle toward the FeCp fragment. In a comparison of **6a** and **7a** with their isolobal analogues, i.e. (η^5-Cp)Fe(CO)(η^3-Cp) and Fe(η^5-Cp)$_2$, respectively, it follows that η^3 coordination to the (η^5-Cp)Fe(CO) fragment is thermodynamically more stable in the case of the ruthena-azadienyl system. The monocarbonyl species (η^5-Cp)-Fe(CO)(η^3-Cp) was only observed in a low-temperature photolysis experiment, involving the conversion of (η^5-Cp)Fe(CO)(η^1-Cp) into ferrocene.[22]

In the RuMn case the starting complex **8** has been smoothly converted into **10**, in which the monoazadienyl ligand is coordinated to the Mn(CO)$_3$ unit via both π bonds. Undoubtedly, this reaction proceeds via the intermediacy of **9** (Figure 5), where only the π(C=C) bond is coordinated to Mn. In the course of this reaction traces of **9** were observed by IR spectroscopy. Under the employed

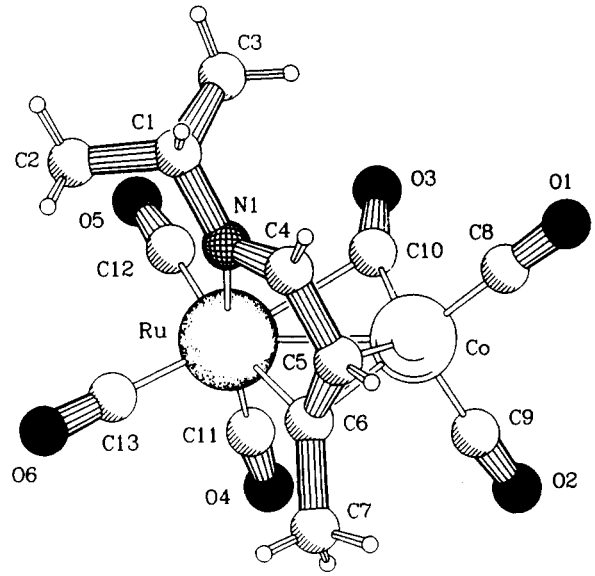

Figure 8. Molecular structure of RuCo(CO)$_6${MeC=C(H)C-(H)=N-*i*-Pr} (**5b**).

reaction conditions, **9**, however, apparently reacts even faster than the starting complex **8**, which means that a thermal reaction is not a proper way of preparing **9**. Therefore, a photochemical route was examined. By irradiation of an hexane solution of **8** indeed moderate amounts of **9** were produced, but now another disturbing side reaction took place, viz. the decomposition of complex **8** into two radical species by homolytic splitting of the intermetallic bond. The $\cdot$Mn(CO)$_5$ radicals then may recombine and form Mn$_2$(CO)$_{10}$, which was isolated. After prolonged irradiation, which is necessary to convert all of complex **8**, only Mn$_2$(CO)$_{10}$ could be isolated.

The RuMn complex **10**, featuring a σ(N),σ(C),π(C=C),π-(C=N)-coordinated monoazadienyl ligand, appeared to be very stable toward both heat and oxidation by air. It also proved to be impossible to prepare **9** by reaction of **10** with CO. Therefore, spectroscopic data for **9** could only be obtained by deduction from spectra of the mixture of **8**–**10**, which was obtained from the reaction of **4** with Mn(CO)$_5^-$ under an inert atmosphere.

Molecular Structure of RuCo(CO)$_6${MeC=C(H)C-(H)=N-*i*-Pr} (5b). The molecular geometry of **5b** is shown in Figure 8, and selected bond distances and angles are given in Table IV. The organometallic compound consists of a Ru(CO)$_3$ fragment and a Co(CO)$_2$ unit, which are linked by a formally single Ru—Co bond of 2.6741 (6) Å. This bond may well be compared to that in other RuCo carbonyl complexes with a formally single Ru—Co bond, as for example to 2.660 (3) Å in CpRuCo(CO)$_3${*t*-BuN=C-(H)C(H)=N-*t*-Bu}.[24] The metal core in **5b** is bridged by a formally monoanionic monoazadienyl ligand and a carbonyl ligand. The bridging character of the carbonyl ligand is not expressed in the M–C bond distances: the Ru–C(10) distance of 2.459 (3) Å can hardly be considered as a bonding interaction, whereas the Co–C(10) bond of 1.766 (3) Å is completely comparable to the Co–C bonds of the two terminally bonded carbonyls (1.756 (4) and 1.790 (4) Å). The Co–C(10)–O(3) angle of 158.0 (3)°, however, deviates considerably from the ideal of 180° for a terminally bonded CO ligand. For this reason C(10)–

(24) Zoet, R.; van Koten, G.; van der Panne, A. L. J.; Versloot, P.; Vrieze, K.; Stam, C. H. *Inorg. Chim. Acta* **1988**, *149*, 177.

Table IV. Selected Bond Distances (Å) and Bond Angles (deg) for 5b (with Esd's in Parentheses)

Ru–Co	2.6741 (6)	Ru–N(1)	2.129 (2)	Ru–C(6)	2.085 (3)
Ru–C(10)	2.459 (3)	Ru–C(11)	1.890 (3)	Ru–C(12)	1.987 (3)
Ru–C(13)	1.900 (4)	Co–C(5)	2.131 (4)	Co–C(6)	2.018 (3)
Co–C(8)	1.756 (4)	Co–C(9)	1.790 (4)	Co–C(10)	1.766 (3)
O(1)–C(8)	1.142 (5)	O(2)–C(9)	1.131 (5)	O(3)–C(10)	1.157 (4)
O(4)–C(11)	1.136 (4)	O(5)–C(12)	1.123 (4)	O(6)–C(13)	1.134 (5)
N(1)–C(1)	1.477 (4)	N(1)–C(4)	1.286 (4)	C(1)–C(2)	1.512 (6)
C(1)–C(3)	1.522 (6)	C(4)–C(5)	1.440 (5)	C(5)–C(6)	1.390 (5)
C(6)–C(7)	1.516 (5)				
C(1)–N(1)–C(4)	118.1 (3)	N(1)–C(1)–C(2)	111.1 (3)	N(1)–C(1)–C(3)	110.4 (3)
C(2)–C(1)–C(3)	112.1 (3)	N(1)–C(4)–C(5)	119.8 (3)	C(4)–C(5)–C(6)	117.4 (3)
C(5)–C(6)–C(7)	122.1 (3)	Ru–C(10)–O(3)	125.3 (2)	Co–C(10)–O(3)	158.0 (3)

O(3) should be considered as an asymmetrically bridging carbonyl ligand, largely localized on Co. Generally a CO bridge is present to strengthen a rather weak intermetallic interaction (compare $Fe_3(CO)_{12}$ and $Ru_3(CO)_{12}$) or to finely counterbalance electronic effects between two metal atoms.[25] The latter reason will apply to the situation in complex **5**, where the electron-rich d^9 Co(0) center is connected to the relatively electron-poor d^7 Ru(I) center. The bridging carbonyl here relieves the charge imbalance between Co and Ru. A similar situation is found for other heteronuclear complexes, such as $CpRuCo(CO)_3$(*t*-Bu-DAB),[24] IrMn- and IrRe–cyclopentadienyl complexes,[26] and complex **6a** (vide infra).

The monoazadienyl ligand in **5b** is formally in the five-electron-donating coordination mode, chelating to Ru and π bonded to Co. The imine bond is not π coordinated to Co, and the C(4)–N(1) bond length of 1.286 (4) Å is comparable to that of other localized C=N bonds in, for example, $Ru_2(CO)_6${C(H)$_2$CC(H)C(H)=N-*t*-Bu} (1.290 (4) Å[27]) and $FeRu(CO)_6${C(H)$_2$CC(H)C(H)=N-*i*-Pr} (1.284 (3) Å[28]). Upon coordination to Co the C(5)–C(6) bond (1.390 (5) Å) is considerably reduced. In $HFeRu(CO)_6${PhC=C(H)C(H)=N-*i*-Pr},[30] however, which represents the only other crystallographically authenticated example of a complex with the monoaza dienyl ligand in the σ(N),σ(C), π(C=C) coordination mode, the C=C bond is reduced to a much larger extent, expressed in the bond length of 1.456 (15) Å. As the reduction of the bond order upon π coordination is generally explained in terms of π back-bonding of the metal into the π^* orbital of the coordinating fragment, this implies that the bonding interaction of the C=C fragment toward a $Co(CO)_3$ unit is much weaker than toward a $Fe(CO)_3H$ fragment.

Molecular Structure of $CpFeRu(CO)_4${PhC=C(H)C(H)=N-*i*-Pr} **(6a).** The molecular geometry of **6a** is shown in Figure 9, and selected bond distances and angles are given in Table V. The structure of complex **6a** contains the heterometallic FeRu metal frame, and the FeRu bond length of 2.6875 (14) Å is indicative of a formally single intermetallic bond.[29] The monoazadienyl ligand is bonded in a five-electron-donating coordination mode, σ(N),σ(C) to Ru and π(C=C) to Fe. The C(6)–C(7) bond of 1.420 (9) Å is comparable to the bond lengths in other

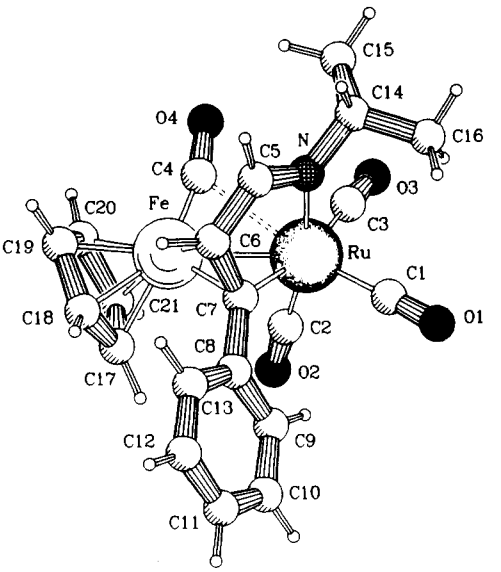

Figure 9. Molecular structure of $(C_5H_5)FeRu(CO)_4$[PhC=C(H)C(H)=N-*i*-Pr} (**6a**).

complexes containing a monoazadienyl ligand in the five-electron-donating coordination mode. The corresponding distance in, for example, $HFeRu(CO)_6$[PhC=C(H)C(H)=N-*i*-Pr} is 1.456 (15) Å.[30]

As in **5b**, the intermetallic bond is bridged by a semibridging carbonyl ligand, C(4)–O(4). Similar to **5b**, the Fe–C(4) bond (1.755 (6) Å) does not deviate from the normal range of bond lengths observed for bonds between Fe and terminal CO ligands (1.74–1.76 Å).[28,30] The angle Fe–C(4)–O(4) (166.8 (6)°), however, does deviate significantly from the ideal 180°; a reason for this feature might be a crystal-packing effect. In the solution IR spectrum of **6a**, however, a weak absorption band is observed in the semibridging-carbonyl region (1880 cm^{-1}), which provides a confirmation of the solid-state structure. On the basis of these data a crystal-packing effect can be ruled out. Considering both the monoazadienyl and cyclopentadienyl ligands in **6a** as formally monoanionic ligands, Ru and Fe both have the formal oxidation state I. Due to the different ligand systems which are attached to each metal, there will be an electronic imbalance between both metal atoms. Therefore, a better explanation seems to be that the difference in electron density between the metal atoms can be counterbalanced more efficiently via the semibridging CO ligand.[25] This effect was also observed for **5b**, where it is even more pronounced due to a larger electronic difference between both metal atoms.

Spectroscopic Analysis of Compounds 5–10. The spectral data for the new complexes are given in Tables VI–VIII. The spectroscopic data for **2a** and **3a** are similar to the data reported for **2b** and **3b**.[5] In the IR spectra of

(25) Cotton, F. A. *Prog. Inorg. Chem.* **1976**, *21*, 1.
(26) Zhuang, J.-M.; Batchelor, R. J.; Einstein, F. W. B.; Jones, R. H.; Hader, R.; Sutton, D. *Organometallics* **1990**, *9*, 2723.
(27) Polm, L. H.; Elsevier, C. J.; Mul, W. P.; Vrieze, K.; Christophersen, M. J. N.; Muller, F.; Stam, C. H. *Polyhedron* **1988**, *7*, 2521.
(28) Beers, O. C. P.; Elsevier, C. J.; Smeets, W. J. J.; Spek, A. L., submitted for publication in *Organometallics*.
(29) Roberts, D. A.; Geoffroy, G. L. In *Comprehensive Organometallic Chemistry*; Wilkinson, G., Stone, F. G. A., Abel, E. W., Eds.; Pergamon: Oxford, England, 1982; Vol. 6, p 803.
(30) Beers, O. C. P.; Elsevier, C. J.; Kooijman, H.; Smeets, W. J. J.; Spek, A. L., submitted for publication in *Organometallics*.

Table V. Selected Bond Distances (Å) and Bond Angles (deg) for 6a (with Esd's in Parentheses)

Ru–Fe	2.6875 (14)	Ru–N	2.138 (6)	Ru–C(1)	1.912 (7)
Ru–C(2)	1.868 (7)	Ru–C(3)	1.959 (7)	Ru–C(4)	2.615 (7)
Ru–C(7)	2.081 (6)	Fe–C(4)	1.755 (6)	Fe–C(6)	2.107 (7)
Fe–C(7)	2.001 (7)	Fe–C(171)	2.097 (16)	Fe–C(181)	2.062 (12)
Fe–C(191)	2.076 (16)	Fe–C(201)	2.071 (13)	Fe–C(211)	2.051 (15)
O(1)–C(1)	1.136 (8)	O(2)–C(2)	1.158 (8)	O(3)–C(3)	1.151 (9)
O(4)–C(4)	1.170 (7)	N–C(5)	1.294 (8)	N–C(14)	1.482 (8)
C(5)–C(6)	1.461 (8)	C(6)–C(7)	1.420 (9)	C(7)–C(8)	1.490 (8)
C(5)–N–C(14)	118.5 (6)	Ru–C(1)–O(1)	177.5 (5)	Ru–C(2)–O(2)	178.2 (6)
Ru–C(3)–O(3)	175.9 (6)	Fe–C(4)–O(4)	166.8 (6)	N–C(5)–C(6)	119.5 (6)
C(5)–C(6)–C(7)	115.2 (5)	C(6)–C(7)–C(8)	120.7 (5)	N–C(14)–C(15)	111.2 (5)
N–C(14)–C(16)	110.0 (6)	C(15)–C(14)–C(16)	112.6 (5)		

Table VI. IR Data[a] for $[Ru(CO)_2Cl\{PhC{=}C(H)C(H){=}N\text{-}i\text{-}Pr\}]_2$ (2a), $Ru(CO)_3Cl\{PhC{=}C(H)C(H){=}N\text{-}i\text{-}Pr\}$ (3a), $RuCo(CO)_6\{RC{=}C(H)C(H){=}N\text{-}i\text{-}Pr\}$ (5a,b), $(C_5H_5)FeRu(CO)_4\{PhC{=}C(H)C(H){=}N\text{-}i\text{-}Pr\}$ (6a), $(C_5H_5)FeRu(CO)_3\{PhC{=}C(H)C(H){=}N\text{-}i\text{-}Pr\}$ (7a), $RuMn(CO)_8\{RC{=}C(H)C(H){=}N\text{-}i\text{-}Pr\}$ (8a,b), $RuMn(CO)_7\{RC{=}C(H)C(H){=}N\text{-}i\text{-}Pr\}$ (9a,b), and $RuMn(CO)_6\{RC{=}C(H)C(H){=}N\text{-}i\text{-}Pr\}$ (10a,b) (a, R = Ph; b, R = Me)

	ν(CO), cm^{-1}						
2a	2079 (m)	2055 (s)	2043 (s)	2010 (w)	1987 (s)	1978 (s)	
3a	2103 (s)	2049 (s)	2012 (s)				
5a	2085 (m)	2028 (vs)	2005 (m)	1983 (s)	1888 (vw, br)[c]		
5b	2083 (m)	2022 (vs)	2010 (m)	1974 (s)	1883 (w, br)[c]		
6a	2057 (s)	1995 (s)	1980 (s)		1880 (m, br)		
7a	2047 (s)	1972 (s)	1966 (s)				
8a	2089 (m)	2047 (vs)	2017 (s)	2007 (s)	1983 (s)	1977 (s)	1967 (m)
8b	2089 (m)	2047 (s)	2011 (s)	1999 (s)	1983 (vs)	1973 (s)	1967 (m)
9a[b]	2080 (s)	2032 (vs)	1985 (s)	1951 (s)			
9b[b]	2090 (s)	1952 (s)					
10a	2075 (m)	2005 (vs)	1995 (s)	1941 (s)	1927 (m)		
10b	2070 (m)	2003 (vs)	1991 (sh)	1989 (m)	1937 (s)	1933 (sh)	

[a] In hexane solution. [b] Recorded in a mixture of **8–10**. Therefore, some absorptions may be masked. [c] When recorded in KBr, the absorption is strong.

Table VII. ^{1}H NMR Data[a] for Compounds 2–10 (a, R = Ph; b, R = Me)

	H_{im}	H_α	*i*-Pr	R	C_5H_5
2a[b]	8.16 (m)	6.35 (m)	5.07/4.87/4.50 (sept, 6.5), 1.56–1.27 (m)	7.38–7.18 (m)	
3a[b]	8.07 (d, 1.5)	6.56 (d, 1.5)	4.00 (sept, 6.5), 1.46/1.44 (d, 6.5)	7.38–7.26 (m)	
5a	8.06 (d, 2.2)	4.51 (d, 2.2)	3.39 (sept, 6.5), 1.17 (d, 6.5)	7.57–7.25 (m)	
5b[c]	7.92 (d, 1.5)	4.15 (d, 1.5)	3.30 (sept, 6.5), 1.09/1.06 (d, 6.5)	3.01 (s)	
6a	7.86 (d, 2.7)	3.60 (d, 2.7)	3.31 (sept, 6.5), 1.08/1.05 (d, 6.5)	7.74–7.10 (m)	4.25 (s)
7a	6.38 (d, 1.9)	5.42 (d, 1.9)	3.41 (sept, 6.5), 1.34/1.25 (d, 6.5)	7.27–7.08 (m)	4.49 (s)
8a	8.09 (d, 2.1)	6.75 (d, 2.1)	4.19 (sept, 6.5), 1.44/1.42 (d, 6.5)	7.35–7.21 (m)	
8b	7.92 (d, 1.6)	6.61 (br)	4.05 (sept, 6.5) , 1.35/1.34 (d, 6.5)	2.73 (d, 1.3)	
9a	8.15 (d, 2.4)	3.37 (d, 2.4)	3.68 (sept, 6.4), 1.22 (d, 6.4)	7.56–7.22 (m)	
9b	7.95 (d, 2.3)	3.09 (d, 2.3)	3.64 (sept, 6.5), 1.21 (d, 6.5)	3.17 (s)	
10a	6.66 (d, 1.8)	5.63 (d, 1.8)	3.14 (sept, 6.5), 1.24/1.23 (d, 6.5)	7.30–7.11 (m)	
10b	6.56 (d, 1.7)	5.24 (br)	3.11 (sept, 6.6), 1.18/1.17 (d, 6.6)	2.44 (s)	

[a] Conditions: δ in ppm, 100.1 MHz, J(H,H) in Hz (in parentheses), $CDCl_3$, 293 K, unless stated otherwise. [b] 300.1 MHz. [c] 263 K.

Table VIII. ^{13}C NMR Data for Compounds 2–10 (a, R = Ph; b, R = Me)

	C_{im}	C_α	C_β	$C_{i\text{-}Pr}$	R	Cp	CO_M[e]	CO_{Ru}
2a[a]	167.9, 167.3	130–125[f]	204.9, 203.6	55.2, 24.7/21.3, 55.0, 24.5/21.0	150.0/149.8, 130–125			198–190
3a[a]	172.5	131.9	209.4	63.9, 23.8/23.6	149.5, 128.9, 128.4, 125.9			191.9, 189.5, 186.6
5a[d]	177.1	72.6	171.0	61.5, 23.8/23.2	150.5, 128.6, 128.0, 127.0		208.1 (br)	194.6, 194.2, 192.3
5b[c]	176.0	75.0	173.9	61.2, 23.5/23.1	34.1		n.o.[g]	193.6, 192.1
6a[c]	179.7	47.4	179.4	59.8, 24.3/23.3	155.5, 128.8, 125.7	82.8	232.1	200.7, 198.2, 193.4
7a[d]	95.5	88.9	160.6	63.1, 29.6/22.9	153.1, 128.7, 127.9, 125.6	73.9		n.o.
8a[a]	165.9	131.2	219.3	60.7, 26.2/23.3	150.3, 128.4, 127.8, 126.3		n.o.	202.0, 199.2, 188.3
8b[b]	165.9	131.2	221.4	60.7, 26.3/22.5	33.2		n.o.	202.1, 198.7, 188.5
9a[b]	178.1	59.3	193.9	60.3, 25.0/23.5	128.8–126.4		n.o.	197.3, 195.4, 194.2
9b[b]	176.7	67.0	195.2	60.4, 25.0/23.7	37.7		n.o.	200.5, 198.3, 196.2
10a[a]	115.2	97.4	182.3	64.2, 28.8/26.1	150.3, 128.9, 128.5, 127.7		224.1	198.1, 194.2, 194.0
10b[a]	114.8	97.6	184.1	64.0, 28.7/25.5	33.5		224.7	199.8, 195.0, 194.1

[a] Conditions: 75.46 MHz, $CDCl_3$, 293 K. [b] Conditions: 75.46 MHz, $CDCl_3$, 263 K. [c] Conditions: 25.1 MHz, $CDCl_3$, 263 K. [d] Conditions: 25.1 MHz, $CDCl_3$, 243 K. [e] M = Fe, Co, Mn. [f] The exact position is masked by Ph resonances. [g] n.o. = not observed.

complexes **5–10** a characteristic absorption pattern in the carbonyl region is observed. Complexes **5** and **6a** both have a semibridging carbonyl ligand, which is found in solution as a weak, broad absorption band at about 1880 cm^{-1}. In KBr this absorption is much stronger, which is a more often encountered phenomenon for bridging carbonyls.[31] From the IR spectra of **5–10** it appears that the wavenumbers of the carbonyl absorptions decrease upon substitution of CO ligands by the π system of the monoazadienyl ligand. This can be explained by the

(31) Mul, W. P.; Elsevier, C. J.; Van Leijen, M.; Vrieze, K.; Spek, A. L. *Organometallics* **1991**, *10*, 533.

inferior π-accepting properties of the monoazadienyl ligand as compared to those of CO, thus enlarging the charge density on the metal and thereby increasing the back-bonding to the carbonyl ligands and hence decreasing the wavenumbers ν(CO). The product of the thermal reaction of **5** (i.e. complex A, Figure 6) also exhibits lower carbonyl wavenumbers than **5**, which is in support of the π,π-coordination mode of the monoazadienyl ligand in A.

The bonding mode of the ligand system can be unambiguously assigned by NMR spectroscopy. In complex **8** the ligand is σ(N),σ(C)-coordinated to Ru and the π bonds are uncoordinated (Figure 5). The resonances of H_{im}/C_{im} and H_α/C_α, for example, in complex **8a** are found at 8.09/165.9 and 6.75/131.2 ppm, respectively, which is in the same range as found for other chelating monoazadienyl ligand systems such as in **2** and **3**.[5] When the coordination mode of the ligand is altered from the formally three-electron-donating to the five-electron-donating σ(N), σ(C)π(C=C) mode, as found in **5**, **6a**, and **9**, the most drastic change in the NMR spectra is observed for the resonances of H_α, C_α, and C_β. All three resonances undergo a low-frequency shift, which can be ascribed to coordination of the C=C bond to the metal and more precisely to π back-donation. The extent of π back-donation depends on the kind of metal center, and this effect can best be interpreted on the basis of the ^{13}C NMR chemical shift of C_α and C_β. The largest low-frequency shift is observed for **6a**, where C_α is found at 47.4 ppm. The value of 59.3 ppm for C_α in **9a** points to s slightly weaker interaction of π(C=C) with the $Mn(CO)_4$ moiety as compared with the Fe(CO)Cp unit. The weakest coordination is observed for **5**, involving C=C coordination to a $Co(CO)_3$ group, where C_α is found at 72.6 ppm. This interpretation of the strength of π coordination toward different metal cores appears to be in agreement with the tendency to change the coordination mode to the formally seven-electron-donating σ(N),σ(C),π(C=C),π(C=N) mode as described above in this paper.

When a CO ligand in **6a** and **9** is substituted by the π(C=N) bond, stable complexes are formed, implying a rather strong bonding interaction. Complex **5**, however, can be thermally converted into a very unstable complex, which cannot even be purified. This is in agreement with the interpretation of the high-frequency resonance of C_α in **5**, also indicating a weak bonding interaction of the $Co(CO)_3$ moiety with the monoazadienyl π system.

A final remark concerns the ^{13}C resonances of the carbonyl groups, which in the case of **5** and **8–10** are broadened or have even not been observed at all (Table VIII). Broadened signals are generally observed for carbon atoms directly bound to metals having nuclear spin $I > 1/2$, such as Mn and Co.[32]

Oxidation Behavior of 5, 7a, 8, and 10. (i) Reaction of 5, 8, and 10 with I_2. In order to assess the strength of the intermetallic bond in **5**, **8**, and **10**, their reactivity toward I_2 was investigated. The reaction of all three types of heterobimetallic complexes with I_2 proceeded very similarly, providing the mononuclear parent complex **3** together with unidentified metal salts, which means that both the RuCo and the RuMn bond are prone to undergo oxidation by I_2 at ambient temperature. It is known that the chain complex $Ru_4(CO)_{10}\{MeC{=}C(H)C(H){=}N\text{-}i\text{-}Pr\}_2$ reacts with I_2 only at elevated temperatures, indicating that there the intermetallic bonds are much more stable.[5]

(32) Aime, S.; Milone, L. *Prog. NMR Spectrosc.* **1977**, *11*, 183.

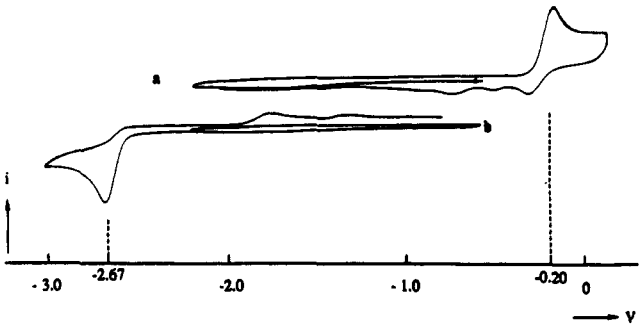

Figure 10. Cyclic voltammograms for complex **7a**: (a) oxidation wave; (b) reduction wave.

(ii) Electrochemistry of Complex 7a. The stability of complex **7a** toward oxidation was examined in electrochemical experiments. In principle this seemed to be promising, as complex **7a** can be regarded as isolobally related to ferrocene, while the Fc/Fc^+ couple is the most common organometallic redox couple.

Complex **7a** in THF can be oxidized at −0.07 V vs Fc/Fc^+ couple. Remarkably, on variation of the scan rate (1, 2, and 5 V/s) i_b/i_f remains constant at a ratio of 0.7, indicating that a complicated, chemically not completely reversible process takes place upon oxidation. Apparently, **7a** decomposes by this oxidation procedure, forming at least three decomposition products, as in the backward scan three reduction peaks are observed (Figure 10a).

One of the decomposition products may be ferrocene, because the cyclic voltammogram, recorded after electrolysis, showed an oxidation/reduction pattern at 0.00 V vs Fc/Fc^+. Controlled-potential electrolysis of **7a** in THF at a potential of −0.05 V beyond $E_{p,a}$ revealed that five electrons are transferred ($n = 4.9$). Assuming that Fe and Ru are both in oxidation state I, full oxidation of both to oxidation state III accounts for the peak current ratio of 3.5 compared to the Fc/Fc^+ couple. This peak current ratio was derived from the CV of **7a** and Fc and thus corresponds to the redox process on a short time scale. Transfer of five electrons, as observed in the relatively long-time-scale electrolysis experiment, may be explained by the additional oxidation of organic material, which is a slower process than metal oxidation. The reduction process is completely irreversible, as can be seen from the CV of **7a** (Figure 10, curve b). A reason for the observed decomposition of **7a** on oxidation may be that the Fe–Ru bond is not stable at the oxidation potential of the first oxidation wave in the CV. This may cause the redox behavior of **7a** to be different from that of ferrocene.

Reactivity of 8 and 10 toward H_2 and Catalytic Hydrogenation with 10a. Aiming at a better understanding of the reactivity of the new heteronuclear complexes and probing their potential for catalytic reactions, we investigated their reactions with H_2. As a monoazadienyl ligand contains unsaturated C=C as well as C=N moieties, the complexes **5–10** constitute, furthermore, potentially interesting models for the study of the chemoselective hydrogenation of C=C and C=N moieties. This approach has already been validated in the study of heteronuclear FeRu complexes.[28,30]

An experiment under an atmosphere of H_2 at 50 °C revealed that complex **8** was unstable under these conditions, resulting in the formation of $Mn_2(CO)_{10}$ and $H_4Ru_4(CO)_{12}$ as main products, due to hydrogenolysis of the Ru–Mn bond and subsequent decomposition of the hydrido fragments.

Scheme I. Proposed Mechanism for the Catalytic Hydrogenation of Styrene by 10a

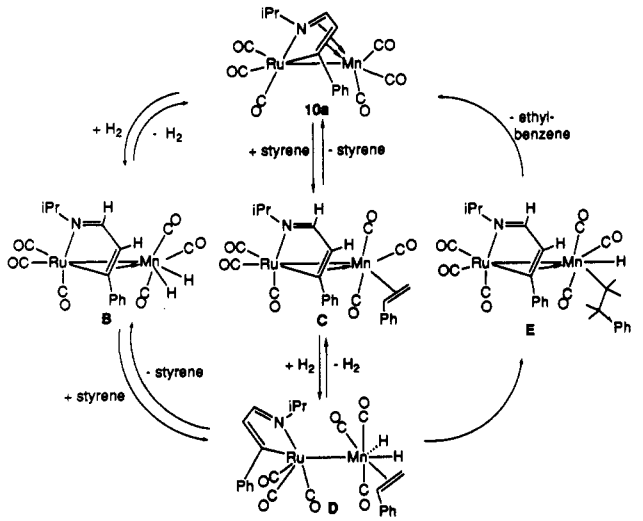

When complex **10** was treated in the same way as **8**, no reaction was observed even at higher temperatures (100 °C).

In principle, open coordination sites can be created in **10** by opening of the π coordination to the Mn atom. As it is apparently stable under H_2, we tested **10** as a homogeneous catalyst for the catalytic hydrogenation of alkenes. At 100 °C styrene could be completely converted into ethylbenzene in 16 h, employing 1.2 bar of H_2 and 1 mol % of catalyst **10a**. Neither the sterically more demanding α-methylstyrene nor the aliphatic 1-octene could be hydrogenated to the corresponding alkane. In the case of 1-octene, only isomerization to the thermodynamically more stable internal octenes was observed.

A mechanism that may explain the catalytic hydrogenation of styrene is presented in Scheme I. A crucial intermediate in this cycle is complex D, featuring a chelating monoazadienyl ligand, a coordinated styrene molecule, and two hydrido ligands. Intermediate D can be formed via two routes. After breaking of the π(C=N) coordination in **10** either H_2 can oxidatively add, forming intermediate B, or styrene can occupy the open site, forming C. By reaction of B with styrene and C with H_2 in both cases D is formed. About the sequence of these reactions we can only speculate. Unfortunately, attempts to demonstrate the actual intermediacy of a dihydrido complex such as B by ^{1}H NMR failed. When complex **10a** was heated to 100 °C, which is the temperature at which the catalytic hydrogenation of styrene proceeds, under 30 bar of H_2 in a high-pressure NMR tube, no sign of hydrido ligands could be observed in the resulting ^{1}H NMR spectrum. Complex **10a** remained completely intact under these conditions.

The starting complex **10a** is recovered by an insertion and a consecutive reductive-elimination step involving intermediate D. The recovery of **10a** after the reaction is in agreement with its presence as a catalytically active species.

An alternative mechanism for the hydrogenation of styrene does not require prior alkene coordination but involves direct insertion of styrene in the Mn–H bond of intermediate B (Scheme I). Such a process has been more commonly proposed, especially in the case of conjugated alkenes such as 1,3-dienes and styrene.[33]

Scheme II. Proposed Mechanism for the Catalytic Isomerization of 1-Octene

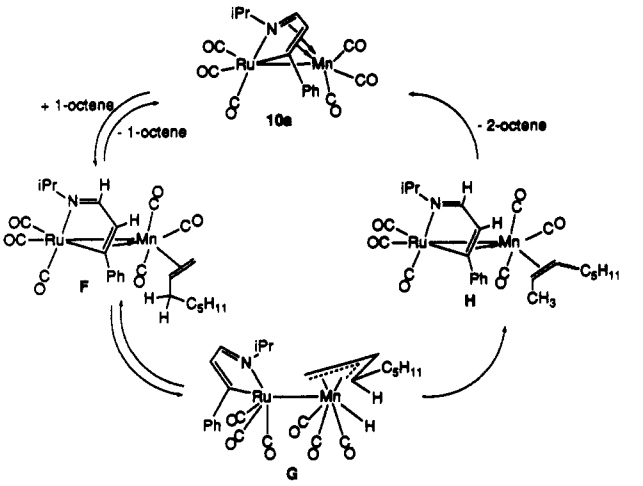

A mechanism for the isomerization of 1-octene, promoted again by complex **10a**, is proposed in Scheme II. The first step is an equilibrium between **10** and intermediate F, as has also been proposed in Scheme I (intermediate C). After creation of the open site by opening of the π(C=N) coordination, a β-H elimination reaction can take place, yielding intermediate G, which features an η^3-allyl-coordinated octenyl ligand and a hydrido ligand. Upon recoordination of the π bonds of the monoazadienyl ligand reductive elimination takes place with the formation of either 1-octene or 2-octene. A similar process starting with the 2-octene so formed may account for the presence of 3-octene. The observed different reactivities of 1-octene and styrene under the same conditions may be explained by assuming that the isomerization process of 1-octene toward internal octenes in an energetically more favorable process than hydrogenation, as is usually encountered in homogeneous hydrogenation of alkenes.[34]

Acknowledgment. The crystallographic part of this work was supported by the Netherlands Foundation for Chemical Research (SON) with financial aid from the Netherlands Organization for Scientific Research (NWO). We thank A. M. Roelofsen and Dr. J. G. M. Van der Linden (Catholic University of Nijmegen) for performing the electrochemical measurements and for helpful discussions and A. J. M. Duisenberg for collection of the X-ray data.

Supplementary Material Available: Thermal motion ellipsoid plots and tables of anisotropic thermal parameters, hydrogen atom parameters, and bond distances and bond angles for **5b** and **6a** and listings of torsion angles and atom coordinates and bond distances and bond angles for the C_5H_5 ring in **6a** (24 pages). Ordering information is given on any current masthead page.

OM920471X

(33) Collman, J. P.; Hegedus, L. S.; Norton, J. R.; Finke, R. G. In *Principles and Applications of Organotransition Metal Chemistry*; University Science Books: Mill Valley, CA, 1987; Chapter 10, p 527.
(34) James, B. R. In *Homogeneous Hydrogenation*; Wiley: New York, 1974.